Since January 2020 Elsevier has created a COVID-19 resource centre with free information in English and Mandarin on the novel coronavirus COVID-19. The COVID-19 resource centre is hosted on Elsevier Connect, the company's public news and information website.

Biomedicine & Pharmacotherapy 109 (2019) 2434–2440

Contents lists available at ScienceDirect

Biomedicine & Pharmacotherapy

journal homepage: www.elsevier.com/locate/biopha

Vascular endothelial growth factor increased the permeability of respiratory barrier in acute respiratory distress syndrome model in mice

Zhao Zhang, Zhouyang Wu, Younian Xu, Dongshi Lu, Shihai Zhang*

Department of Anesthesiology, Union Hospital, Tongji Medical College, Huazhong University of Science and Technology, China

ARTICLE INFO

Keywords:
Lipopolysaccharide
Acute respiratory distress syndrome
Vascular endothelial growth factor
Alveolar epithelial cell
Tight junction

ABSTRACT

Background: Acute respiratory distress syndrome is associated with a mortality of 45%. The authors investigated the possible mechanisms and effect of vascular endothelial growth factor on alveolar epithelial barrier permeability in acute respiratory distress syndrome mice model.

Methods: Eighty Male BALB/c mice were randomly assigned to four group: PBS group, LPS group, sFlt group, or LPS + sFlt group. The levels of vascular endothelial growth factor and total protein in bronchoalveolar lavage fluid were compared, together with lung injury score and the histopathology of alveolar epithelial barrier. The expressions of vascular endothelial growth factor and tight junction proteins mRNA in lung tissue were also studied.

Results: Lipopolysaccharide (LPS) inhaling was accompanied with increasing lung vascular endothelial growth factor (VEGF) expression. Anti-VEGF with soluble fms-like tyrosine kinase-1 (sFlt-1) attenuated the lung injury effectively.

Conclusions: Our data indicate that anti-vascular endothelial growth factor with soluble fms-like tyrosine kinase-1 could maintain the normal structure and function of respiratory membrane in acute respiratory distress syndrome mice model and might be a suitable therapeutic tool for the treatment of acute respiratory distress syndrome.

1. Introduction

Acute respiratory distress syndrome (ARDS) has an incidence of 86 cases per 100, 000 person-years and is associated with a mortality of around 45% [1,2]. The syndrome is characterized by diffuse capillary barrier damage and increasing respiratory membrane permeability. It has been reported that the basic pathological change may give rise to consecutive pulmonary edema, gas exchange disorder, and respiratory distress [1]. Since increasing respiratory membrane permeability is the basic pathological change, the most critical aspect in ARDS therapy becomes how to decrease the respiratory membrane permeability. However, there is still no effective treatment to reduce the respiratory permeability to date.

Vascular endothelial growth factor (VEGF) is expressed in several parts of lung and may play an important role in ARDS [3]. As a potent angiogenic factor, it has been reported that VEGF increases microvascular permeability by 20, 000 times more potently than histamine [4,5]. Nevertheless, the mechanism of the impact of VEGF on respiratory membrane permeability in ARDS is still unclear and further investigation in this area is definitely still needed which motivated the present research work.

2. Material and methods

2.1. Animals and sample treatment

Ethical approval for this investigation was obtained from the Institutional Animal Care and Use Committee at Tongji Medical College, Huazhong University of Science and Technology (IACUC Number: 354). All animal experiments complied with the ARRIVE guidelines.

Male BALB/c mice of 4–6 weeks (20 ± 2 g) old were obtained from Animal Center of Tongji Medical College. They were kept in an animal facility for at least 3 days prior to experiments to allow adaptation to the environment and confirmation of their health. The animals were maintained on a light-dark cycle with light from 8: 00 to 20: 00 at 25 °C. Each animal received rodent laboratory chow and water ad libitum. All experiments were approved by the animal care committee. Eighty mice

* Corresponding author at: Department of Anesthesiology, Union Hospital, Tongji Medical College, Huazhong University of Science and Technology, 1277 Jiefang Avenue, Wuhan 430022, China.
E-mail address: 9377827@qq.com (S. Zhang).

https://doi.org/10.1016/j.biopha.2018.11.132
Received 14 June 2018; Received in revised form 26 November 2018; Accepted 27 November 2018

Table 1
Levels of lung injury in four groups (n = 80).

group	pH	PaO_2(mmHg)	$PaCO_2$(mmHg)	Lung injury score
PBS	7.42 ± 0.07	97.3 ± 9.0	37.8 ± 5.8	1.5(0–3)
sFlt	7.41 ± 0.06	96.6 ± 8.5	33.2 ± 7.6	1.5(0–3)
LPS	7.17 ± 0.05**	64.2 ± 10.5**	49.0 ± 9.2*	12(8–14)**
LPS + sFlt	7.29 ± 0.07*#	84.3 ± 7.2*# #	36.5 ± 4.8#	6(5–7)*#

PaO_2 = partial pressure of oxygen; $PaCO_2$ = partial pressure of carbon dioxide; Data are $x \pm$ SD or medians with ranges in the brackets. * $P < 0.05$ or ** $P < 0.001$ compared with controls; and # $P < 0.05$ or # # $P < 0.001$ compared with LPS group.

were divided into 4 groups with 20 mice in each group randomly assigned, i.e., PBS group, LPS group, sFlt [6] (soluble vascular endothelial cell growth factor receptor-1) group, and LPS + sFlt group. All animals were anesthetized using pentobarbital sodium (40 mg/kg, i.p.). The mice in the LPS group and the LPS + sFlt group were intratracheally instilled via tracheal tube (IV Catheter 24 G, BD Insyte, Suzhou, China) with 3 mg/kg LPS as used in the literatures [7,8], (2 mg/mL, *Escherichia coli* 055: B5, Sigma Chemical, St. Louis, MO, USA). The mice in the PBS group and the sFlt group were instilled with equal volume of PBS. Right after LPS or PBS administration, recombinant mouse sFlt-1-Fc fusion protein 50 μg/kg (5 μg/ml) [6] was infused via tail vein to each mouse in the sFlt and the LPS + sFlt group. The mice in the PBS and LPS groups were given equal volume of PBS as control.

For each mouse, the model was prepared and held for 24 h before the blood sample was collected and stored in a heparinized tube using left ventricular puncture technique. Blood gas analysis was carried out with a blood gas analyzer (ABL700, Radiometer Co., Copenhagen, Denmark). Immediately after cardiac puncture, the mouse was killed by exsanguination and the thorax was opened with a midline thoracotomy and a tracheal tube was inserted again [9]. The lungs were lavaged 3 times thereafter with 0.8 ml aliquots of normal saline at room temperature to collect bronchoalveolar lavage fluids (BALF). The BALF fluids were centrifuged to obtain the supernatants which were stored at −20 °C for future measurement [9]. The left lung was cut off and then was snap frozen in liquid nitrogen until subsequent analysis. The right upper lobes of the lungs were harvested and immersed in 10% formalin until processing in paraffin wax for histopathological examination. The right lower lobes of the lungs were fixed with glutaraldehyde and 4% phosphate solution mixture [9].

2.2. Total protein and VEGF levels in BALF

Total protein concentration in the BALF was determined using a bicinchoninic acid assay kit (P0010S, Beyotime biotechnology, Nantong, Jiangsu province, China) [10]. The optical densities were recorded using an enzyme mark instrument (SPECTRAMAX 190, Molecular Devices Corp., Sunnyvale, CA, USA) at 450 nm wavelength. A standard curve was thus generated to calculate the protein concentrations in BALF.

The VEGF level in BALF was determined using an enzyme-linked immunosorbent assay kit for mouse VEGF according to manufacturer's instruction (MMV00, R&D Systems incorporation, Minneapolis, MN, USA) [11]. A specific monoclonal antibody was precoated onto a microplate before a sample was pipetted into the well. A polyclonal detection antibody was added subsequently prior to addition of the substrate solution to the well. The optical density developed in proportion to the amount of specific cytokine was recorded using an enzyme mark instrument (SPECTRAMAX 190, Molecular Devices Corporation, Sunnyvale, CA, USA) at 450 nm wavelength. A standard curve was then generated to calculate the concentrations of VEGF in BALF.

2.3. Real time quantitative PCR for detection of VEGF, occluding, and ZO-1 mRNA expression in lung tissue

Total RNA was isolated from lung tissues using the Trizol reagent (15596-026, Sigma Chemical, St. Louis, MO, USA) according to the manufacturer's protocol [12,13]. First-strand complementary DNA (cDNA) was synthesized using oligo (dT18) and M-MLV reverse transcriptase (M1701, Promega Corporation, Madison, WI, USA). Target gene 1 (VEGF: forward primer, 5′-GTAACGATGAAGCCCTGGAGTG-3′; reverse primer, 5′-CGTCTGCGGATCTTGGACAAAC-3′), Target gene 2 (occluding: forward primer, 5′-ACT GGG TCA GGG AATATC CA-3′; reverse primer, 5′-TCA GCA GCA GCC ATG TAC TC-3′), target gene 3 (ZO-1: forward primer, 5′-ACT CCC

ACT TCC CCAAAAAC-3′; reverse primer, 5′−CCACAG CTG AAG GAC TCA CA-3′), and reference gene (β actin: forward primer, 5′-TGC TGT CCC TGT ATG CCT CTG-3′; reverse primer, 5′-CTT TGA TGT CAC GCA CGA TTT C-3′) were generated and optimized to an equal annealing condition. The fold change in the target gene, normalized to β-actin and relative to the expression at time zero, was calculated for each sample using the following equation: Fold = $2^{-(\triangle Ct\ control - \triangle Ct\ sample)}$.

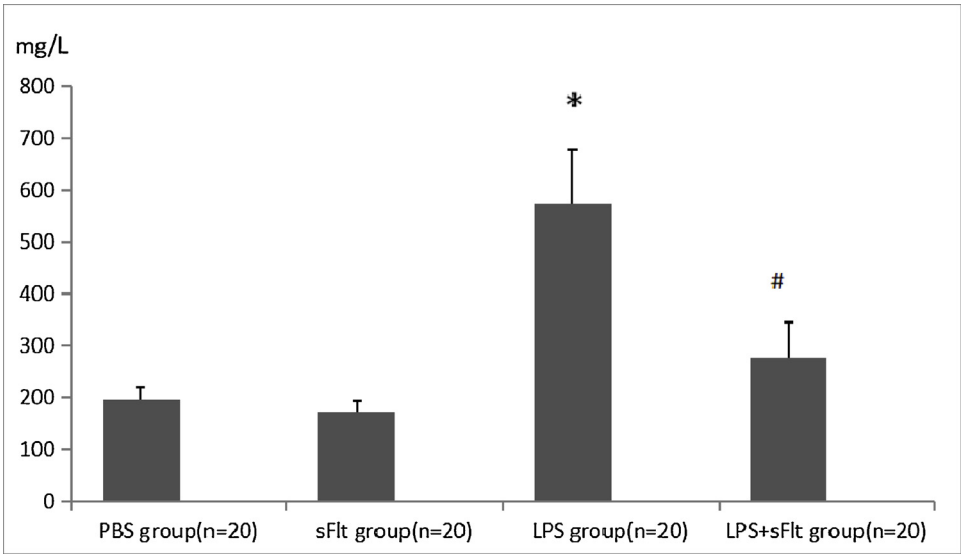

Fig. 1. The level of total protein in BALF.
* $P < 0.05$ compared with PBS group, # $P < 0.05$ compared with LPS group.

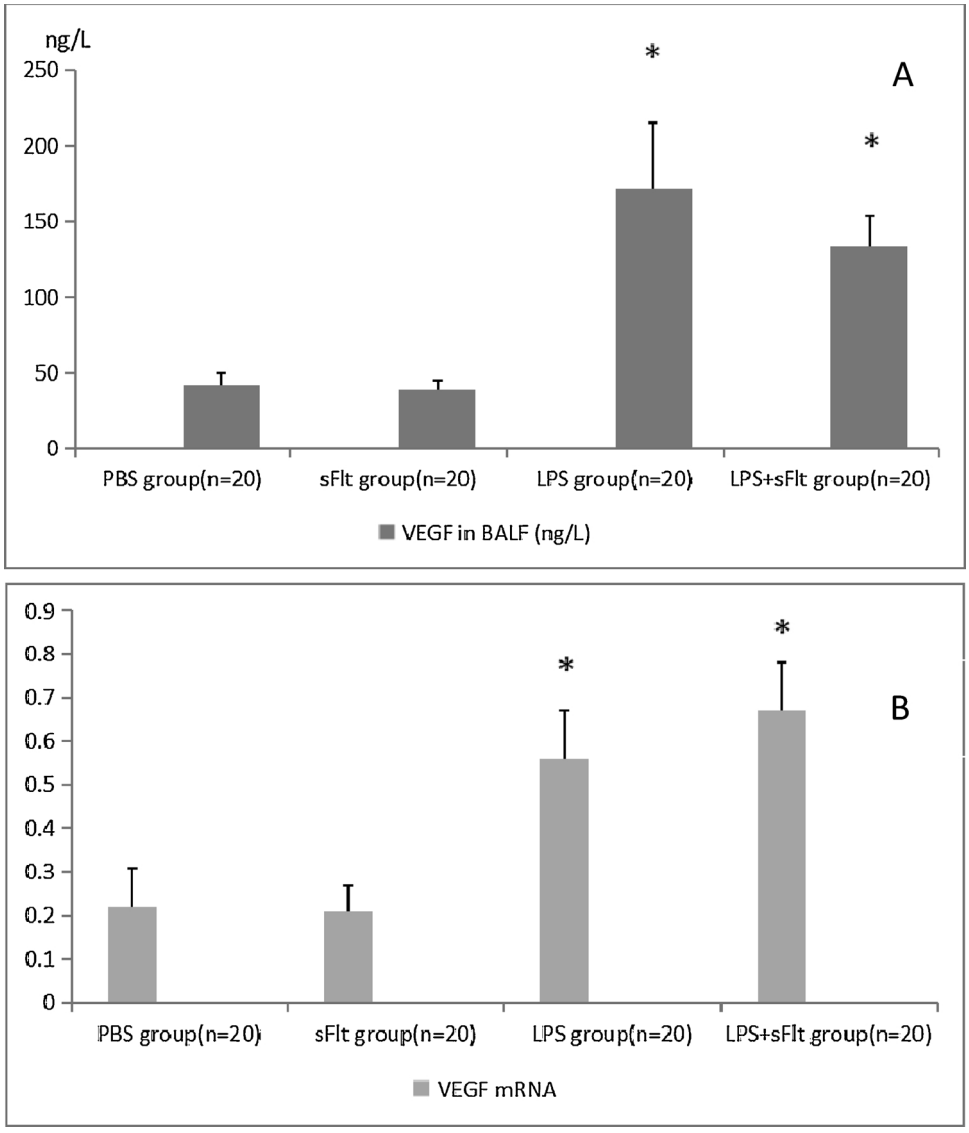

Fig. 2. The levels of VEGF in BALF and VEGF mRNA in lung tissue.
A, the content of VEGF in BALF of different groups were different. B, Data were expressed as a ratio of VEGF mRNA in BALF to actin expression. * $P < 0.05$ compared with PBS group, # $P < 0.05$ compared with LPS group.

2.4. Histopathological examination

Paraffin sections (5 μm) were adhered to slides and stained with hematoxylin and eosin (H&E). The slides were then examined with light microscope. Two blinded pathologists were employed to score lung injury based on the following four factors, namely, alveolar congestion, hemorrhage, infiltration, aggregation of neutrophils in air or vessel wall, and thickness of alveolar wall/ hyaline membrane formation. Each factor was graded at five point scales based on the previous report [7], i.e., 0 for minimal (little) damage, 1 for mild damage, 2 for moderate damage, 3 for severe damage, and 4 for maximal damage. A consensus of the diagnosis of lung injury score was independently conducted by the two experienced pathologists. An area was re-evaluated until the results were in line with each other. Finally, a total lung injury score was calculated as the sum of the four factors. As a result, the minimum and maximum possible scores were 0 and 16, respectively.

2.5. Electronmicroscope examination

The biopsy materials were fixed with a mixture of glutaraldehyde and 4% phosphate solution [12]. Phosphate solution and osmium tetroxide were used for post fixation. Sections of 600–700 Å thickness were obtained from the polymerized material with ReichertUM2. The sections stained with uracyl acetate and lead citrate were examined using an electron microscope (Tecnai G2 12, FEI Co., Eindhoven, Holland).

2.6. Statistical analysis

Data were expressed as means ± S.D. except for lung injury scores which were represented as median (range). Statistical analysis was conducted using SPSS 22.0 for windows (SPSS Co., Ltd., Chicago, IL). The lung injury scores were analyzed using the Kruskal-Wallis rank test followed by Mann-Whitney U test. The other data were analyzed by one-way analysis of variance (ANOVA).

3. Results

3.1. Blood gas analysis and lung injury score

Table 1 shows the levels of lung injury of the 80 mice in four groups

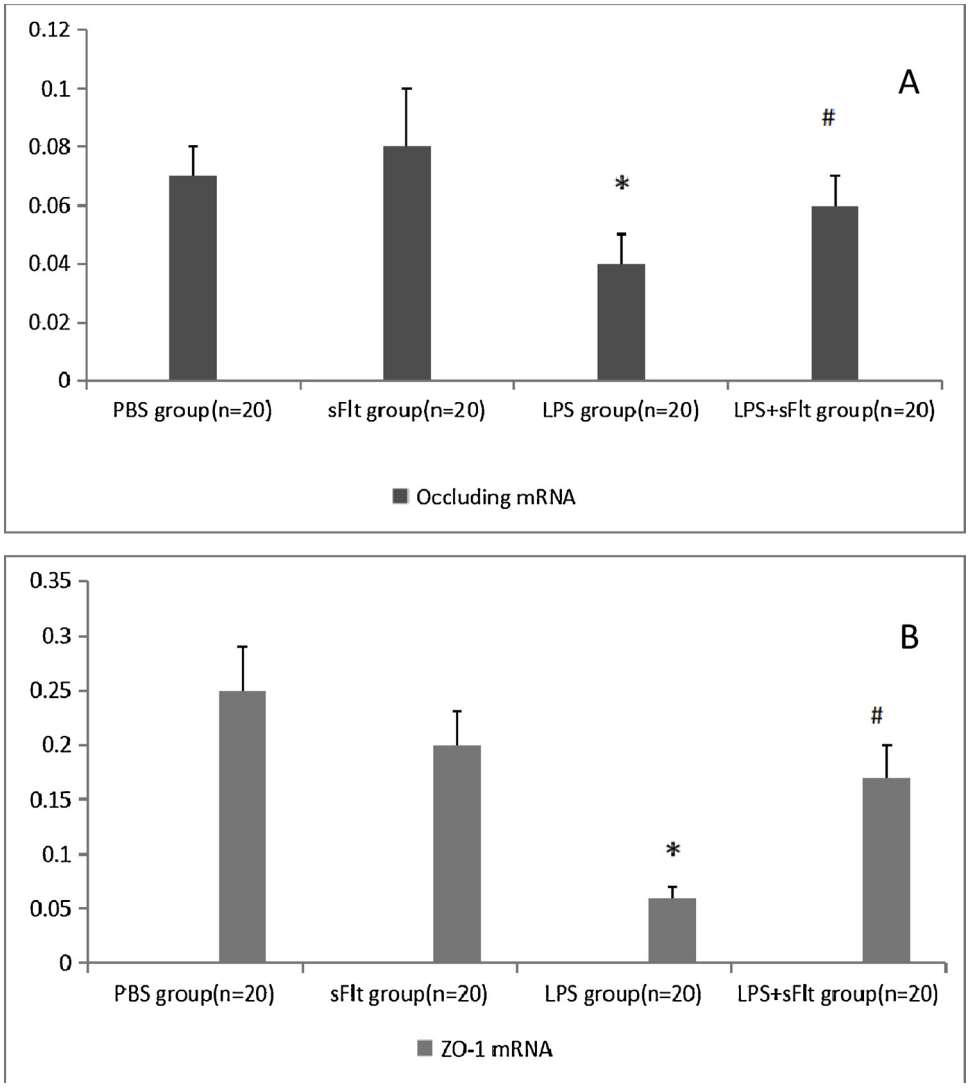

Fig. 3. Expressions of occluding and ZO-1 mRNA.
Data were expressed as a ratio relative to actin mRNA expression, * P < 0.05 compared with PBS group, # P < 0.05 compared with LPS group.

examined in this work. Control animals injected with PBS or sFlt-1 showed normal PaO_2, $PaCO_2$, BALF protein, and lung injury score. LPS challenge caused acidosis, hypoxia, carbon dioxide accumulation, and increased lung injury score. BALF protein levels in the LPS group increased significantly. sFlt-1 administration improved acidosis, hypoxia, carbon dioxide accumulation considerably. Lung injury score and protein levels in BALF were also improved in the LPS + sFlt group.

3.2. Levels of total protein in BALF

As shown in Fig. 1, the level of protein in BALF in the LPS group is the highest comparing with the PBS and sFlt groups ($P < 0.05$), while the BALF protein level in the LPS+ sFlt group is substantially lower than that of the LPS group ($P < 0.05$).

3.3. The expressions of VEGF in BALF and VEGF mRNA in lung tissue

Fig. 2A shows that the BALF VEGF levels in the LPS group and the LPS + sFlt group are much higher than those of the control groups ($P < 0.05$), The same trend was observed for the VEGF mRNA level as shown in Fig. 2B. However, the difference in the VEGF mRNA level between the LPS group and the LPS + sFlt group was not significant. Similarly, the difference in the VEGF in BALF between the above two groups is irrelevant.

3.4. The expressions of occluding and ZO-1 mRNA in lung tissue

Fig. 3 shows the impact of LPS challenge on the occluding and ZO-1 mRNA expressions in lung tissue. It is clear that LPS challenge results in significant decrease in both occluding mRNA (Fig. 3A) and ZO-1 mRNA (Fig. 3B) while the effect at the presence of LPS + sFlt group improves.

3.5. Light microscopy and lung injury score

Fig. 4 shows the results of histopathological examination of lung tissues. Fig. 4A (PBS group) and Fig. 4B (sFlt group) exhibit normal lung histology. Fig. 4C (LPS) indicates extensive morphological lung damage with LPS treatment, such as edema, thickening of the alveolar walls, and infiltration of inflammatory cells into alveolar and interstitial spaces. There is also lung damage with the LPS + sFlt group (Fig. 4D) although the damage degree is not as serious as that of the LPS group ($P < 0.05$). These observations are consistent with the lung injury scores as can be seen in Table 1.

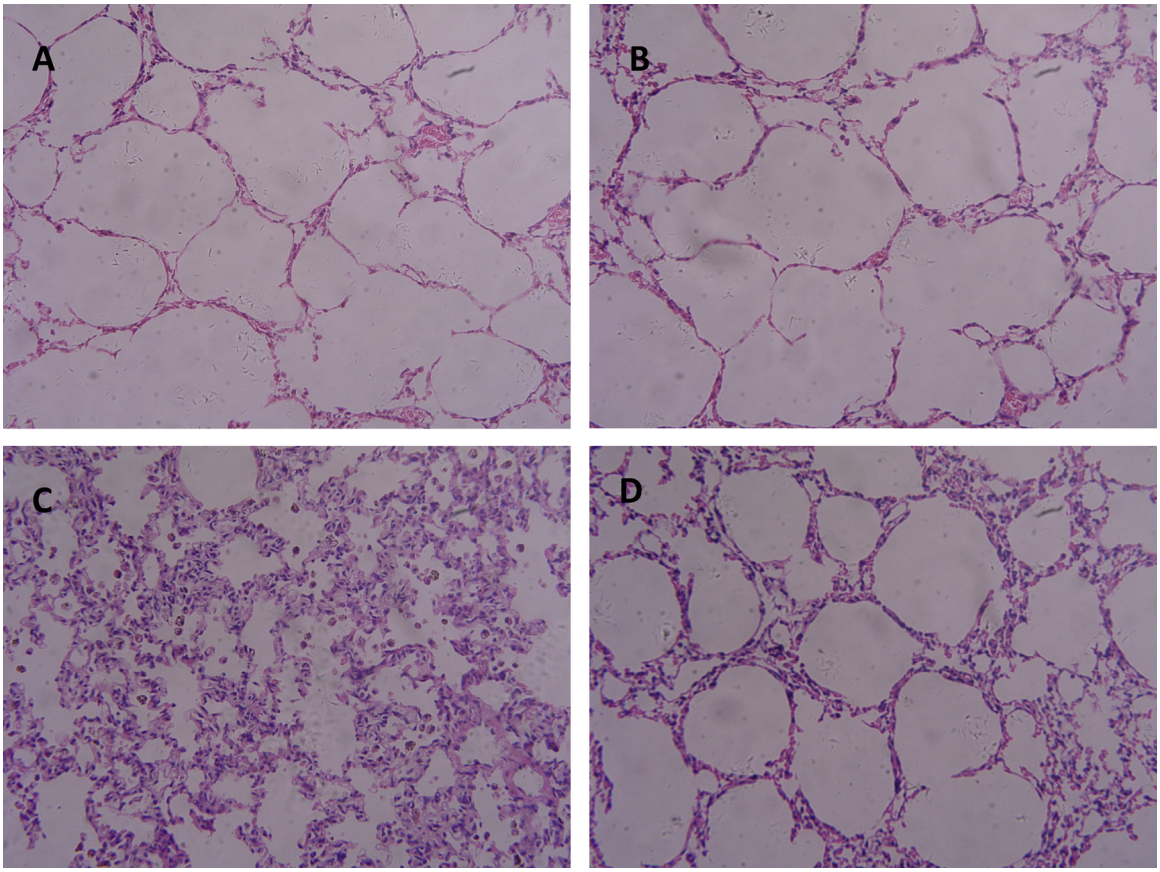

Fig. 4. Results of histopathological examination of lung tissues (H-E, × 200). A: PBS group ; B: sFlt group ; C: LPS group ; D: LPS + sFlt group.

3.6. Lung electron microscope examination

Tight junctions of type I alveolar epithelial cells were observed by electron microscopic examination of the lung in mice. Figs. 5A and B show the intact alveolar-capillary membrane for the PBS group and the sFlt group, respectively. In contrast, as indicated in Fig. 5C, the introduction of LPS challenge induced the disruption of tight junctions between alveolar epithelial cells, type I alveolar epithelial cell shrinkage and detachment from the basement membrane, thickening of the alveolar–capillary membrane, and infiltration of cellulose into alveolar. Nevertheless, sFlt-1 administration attenuated the disruption of tight junctions and the thickening of alveolar–capillary membrane (Fig. 5D).

4. Discussion

The research work reported here intends to clarify four issues. Firstly, LPS inhaling is expected to help set up an applicable ARDS model. As has been addressed previously, LPS intratracheal instillation brought about hypoxia, carbon dioxide accumulation, and increased lung injury score. The ARDS model is characterized by increased permeability of alveolar-capillary barrier and extensive morphological lung damage, such as edema, incrassation of the alveolar wall, and infiltration of inflammatory cells into alveolar and interstitial spaces. This model is fully consistent with the etiology, pathophysiology and clinical characteristics of ARDS [1,2]. Secondly, LPS inhaling was accompanied with increasing lung VEGF expression (both VEGF mRNA in lung tissue and VEGF expression in BALF). Thirdly, Anti-VEGF with soluble fms-like tyrosine kinase-1 (sFlt-1) attenuates the lung injury effectively (lung injury score and protein quantification in BALF). Fourthly, VEGF may cause lung injury through inhibiting the expression of tight junction proteins (occludin and ZO-1).

There are still confusions to some degree about the role of VEGF in ARDS. An in vitro research [13] indicated that the expression of VEGF in airway epithelial cell lines could be augmented by Interleukin-1 beta (IL-1β), tumour necrosis factor-alpha (TNF-α), lipopolysaccharide (LPS), interferon-gamma (IFN-ϒ), smoke extract (SE), and neutrophil elastase (NE) stimulation. Clinical data [14], yet, suggest a significant correlation between the plasma VEGF level and the lung injury score. The work by Song et al [15] showed VEGF might contribute to vascular endothelial repair and function as a protective factor during the recovery period (7 days) of ARDS. In this work, the models were observed for 24 h and significant improvement has been achieved suggesting that generalization that VEGF is beneficial or harmful should be avoid as it may depend on the stage of inflammation development. It can be concluded that anti-VEGF therapy should be practiced as early as possible in ARDS.

The affect mechanism of VEGF on ARDS is still unclear at present time. Kiichiro's research [16] showed that adenovirus-mediated overexpression of VEGF exacerbated the LPS-mediated toxic effects. Overexpression of sFlt-1 attenuated the rise of VEGF levels and blocked the effect of endotoxemia on cardiac function, vascular permeability, and mortality. However this research did not investigate the mechanism of antagonizing VEGF to reduce mortality. Tight junction proteins such as occludin and ZO-1 had been identified to be the downstream molecules of VEGF in regulating permeability [17]. Our work indicated that the increased VEGF participated in the damage of three layer structure of respiratory barrier through tight junction proteins such as occludin and ZO-1. Anti-VEGF with sFlt-1 could increase the expression of tight junction proteins, repair the alveolar epithelial barrier, and improve the gas exchange function of ARDS model.

Previous studies [15,18,19] have shown that VEGF played an

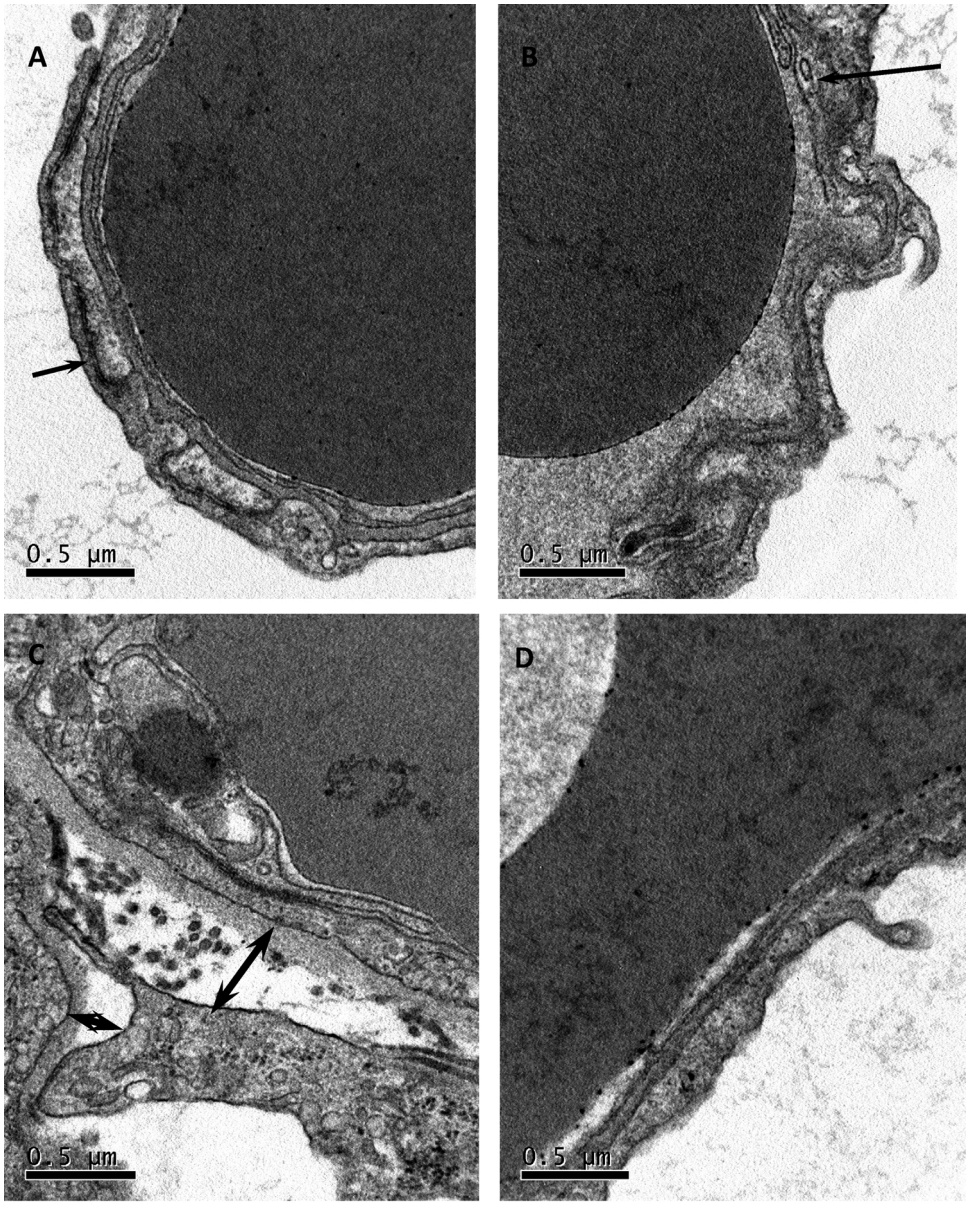

Fig. 5. Electronmicroscopic examination.
A: PBS group, B: sFlt group, C: LPS group, D: LPS + sFlt group.
Arrows indicate tight junctions between alveolar epithelial cells. The tight junctions between alveolar epithelial cells are normal in the PBS group and are broken in the LPS group. The tight junctions between alveolar epithelial cells are widened.

important role in the pathogenesis of inflammation. Anti-VEGF attenuated the lung damage and decreased the infiltration of inflammatory cells. From the histopathological examination of lung tissues in our study (Fig. 4), it can be summarized that infiltration of inflammatory cells into alveolar in the ARDS model and anti-VEGF decreased the infiltration. These evidences suggest that VEGF may increase the permeability of respiratory membrane leading to promoted lung injury through inflammatory cascade. More research work is definitely needed to draw an unblemished conclusion, though.

5. Conclusions

Our research indicates that anti-VEGF with sFlt-1 could maintain the normal appearance and function of the respiratory barrier and might be a suitable therapeutic tool for the treatment of ARDS.

Formatting of funding sources

This study was supported by Young Scholar Research Grant of Chinese Anesthesiologist Association to Zhao Zhang [grant number: 21700007].

Consent for publication

Not applicable.

Declarations of interest

None.

Acknowledgements

We want to thank Prof Heping Guo and Prof Jinghui Zhang for their technical assistance

References

[1] J.R. Beitler, D.A. Schoenfeld, B.T. Thompson, Preventing ARDS: progress, promise, and pitfalls, Chest 146 (4) (2014) 1102–1113.
[2] G.D. Rubenfeld, E. Caldwell, E. Peabody, J. Weaver, D.P. Martin, M. Neff, E.J. Stern, L.D. Hudson, Incidence and outcomes of acute lung injury, N. Engl. J. Med. 353 (2005) 1685–1693.
[3] E.E. Faridy, S. Permutt, R.L. Riley, Effect of ventilation on surface forces in excised dogs' lungs, J. Appl. Physiol. 21 (1966) 1453–1462.
[4] R.G. Spragg, J.F. Lewis, H.D. Walmrath, J. Johannigman, G. Bellingan, P.F. Laterre, M.C. Witte, G.A. Richards, G. Rippin, F. Rathgeb, D. Häfner, F.J. Taut, W. Seeger, Effect of recombinant surfactant protein C–based surfactant on the acute respiratory distress syndrome, N. Engl. J. Med. 351 (2004) 884–892.
[5] N. Ferrara, VEGF: an update on biological and therapeutic aspects, Curr. Opin. Biotechnol. 11 (6) (2000) 617–624.
[6] B.K. Zebrowski, S. Yano, W. Liu, R.M. Shaheen, D.J. Hicklin, J.B. Putnam Jr, L.M. Ellis, Vascular endothelial growth factor levels and induction of permeability in malignant pleural effusions, Clin. Cancer Res. 5 (11) (1999) 3364–3368.
[7] H.J. Schoch, S. Fischer, H.H. Marti, Hypoxia-induced vascular endothelial growth factor expression causes vascular leakage in the brain, Brain 125 (2002) 2549–2557.
[8] N.F. Voelkel, R.W. Vandivier, R.M. Tuder, Vascular endothelial growth factor in the lung, Am. J. Physiol. Lung Cell Mol. Physiol. 290 (2) (2006) L209–221.
[9] A.R. Medford, A.B. Millar, Vascular endothelial growth factor (VEGF) in acute lung injury (ALI) and acute respiratory distress syndrome (ARDS): paradox or paradigm? Thorax 61 (7) (2006) 621–626.
[10] P.N. Tsao, F.T. Chan, S.C. Wei, W.S. Hsieh, H.C. Chou, Y.N. Su, C.Y. Chen, W.M. Hsu, F.J. Hsieh, S.M. Hsu, Soluble vascular endothelial growth factor receptor-1 protects mice in sepsis, Crit. Care Med. 35 (2007) 1955–1960.
[11] T. Nagase, N. Uozumi, S. Ishii, K. Kume, T. Izumi, Y. Ouchi, T. Shimizu, Acute lung injury by sepsis and acid aspiration: a key role for cytosolic phospholipase A2, Nat. Immunol. 1 (1) (2000) 42–46.
[12] H.E. Barker, J.T. Paget, A.A. Khan, K.J. Harrington, The tumour microenvironment after radiotherapy: mechanisms of resistance and recurrence, Nat. Rev. Cancer 15 (7) (2015) 409–425.
[13] S. Boussat, S. Eddahibi, A. Coste, et al., Expression and regulation of vascular endothelial growth factor in human pulmonary epithelial cells, Am. J. Physiol. Lung Cell Mol. Physiol. 279 (2000) L371–378.
[14] F. Hua, X. Wang, L. Zhu, Terlipressin decreases vascular endothelial growth factor expression and improves oxygenation in patients with acute respiratory distress syndrome and shock, J. Emerg. Med. 44 (2) (2013) 434–439.
[15] J. Song, H. Lu, X. Zheng, X. Huang, Effects of vascular endothelial growth factor in recovery phase of acute lung injury in mice, Lung 193 (December (6)) (2015) 1029–1036.
[16] Y. Kiichiro, C.L. Patricia, M.M. Janet, Vascular endothelial growth factor is an important determinant of sepsis morbidity and mortality, J. Exp. Med. 203 (2006) 1447–1458.
[17] L. Zhang, H. Liu, Y.M. Peng, Y.Y. Dai, F.Y. Liu, Vascular endothelial growth factor increases GEnC permeability by affecting the distributions of occludin, ZO-1 and tight juction assembly, Eur. Rev. Med. Pharmacol. Sci. 19 (14) (2015) 2621–2627.
[18] M. Shibuya, VEGF-VEGFR system as a target for suppressing inflammation and other diseases, Endocr. Metab. Immune Disord. Drug Targets 15 (2) (2015) 135–144.
[19] D. Karmpaliotis, I. Kosmidou, E.P. Ingenito, K. Hong, A. Malhotra, M.E. Sunday, K.J. Haley, Angiogenic growth factors in the pathophysiology of a murine model of acute lung injury, Am. J. Physiol. Lung Cell Mol. Physiol. 283 (September (3)) (2002) L585–95.